

Dependence of Charge-Transport Parameters on Static Correlation and Self-Interaction Energy: The Case of a 1,4-Bis(Phenylethynyl)Benzene Derivative Conjugated Molecule

J. C. Sancho-García* and A. J. Pérez-Jiménez†

Departamento de Química Física, Universidad de Alicante, E-03080 Alicante, Spain

Received: March 12, 2008; Revised Manuscript Received: July 30, 2008

The current research on molecular-based devices built with highly unsaturated molecules is largely assisted by computational techniques. These modern computational tools are intended to serve (i) to understand the relation between the mechanism of charge transport and the chemical composition of the semiconductors and (ii) to perform the molecular engineering needed to design new and more efficient organic materials. We have studied the case of a rod-shaped conjugated molecule widely used in molecular electronics. The results of multireference perturbation theory up to second order (MRMP2) and complete active space self-consistent field calculations (CASSCF) are compared with the results provided by energy density functionals. Motivated by the diverse accuracy of the results depending on the theoretical method selected, we have systematically studied the physical origin of the discrepancies. We find that a subtle interplay between correlation effects and the self-interaction energy mainly governs the results, which makes it thus difficult to anticipate the quality of a method without knowing in advance its dependence on both effects. We thus encourage careful testing of computational methods for the rational design and understanding of conjugated materials for charge conduits.

1. Introduction

Electronic structure calculations for single molecules are usually a prerequisite for the application of theoretical models, such as the recent polaron formation model,^{1,2} to the understanding of electronic transport on molecular junctions because they are key to interpret and/or estimate the charging processes and conformational changes that may be induced on the molecule acting as the molecular bridge. Two magnitudes that quantify both effects for an organic molecular semiconductor are the internal hole reorganization energy (λ^{*+}) and torsional barrier height (ΔE_{tors}) between stable conformers. The former represents the energy gained by geometric relaxation after hole arrival to the cation equilibrium structure and can be defined as^{3–5}

$$\lambda^{*+} = E_{M^{*+}/M} - E_{M^{*+}} \quad (1)$$

with $E_{M^{*+}}$ being the energy of the charged molecule (radical cation, doublet) at its optimum geometry and $E_{M^{*+}/M}$ being the energy of the charged molecule but at the optimized geometry of the neutral (singlet) molecule. The excess charge is known to produce a geometry distortion over a section of the conjugated core.^{6–8} On the other hand, ΔE_{tors} is taken as the energy difference between optimized structures of a planar (on) and a perpendicular (off) conformation.⁹

Our main objective in this work is to elucidate the extent to which theoretical methods are able to accurately predict the magnitude of both properties. We are aimed at establishing useful guidelines for a better interpretation of the results obtained with different methods currently in use by finding, measuring, and, if possible, correcting the causes behind their observed deficiencies. In particular, by means of ab initio multiconfigurational and density functional theory (DFT) calculations, we

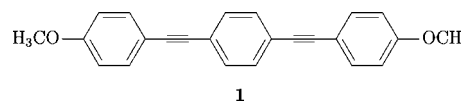


Figure 1. Chemical structures of the 1,4-bis(phenylethynyl)benzene derivative. The hydrogen atoms on the central core have been omitted for clarity.

will be able to analyze the influence of subtle electronic effects, such as static correlation and self-interaction energy, on the hole-transport properties of a semiconducting molecular wire. As a molecular prototype^{10,11} for this study, we choose the rigid rod-shaped conjugated molecule shown in Figure 1, an oligo(phenylene ethylene) which has been thoroughly investigated during the last years^{12,13} and for which experimental estimates of both properties have recently become available. In fact, the gas-phase experimentally determined hole reorganization energy of **1** (0.30 ± 0.05 eV)¹⁴ is comparable to that of the bistriarylamine derivative tetraphenyldiaminobiphenyl (TPD),¹⁵ a well-established hole-transport material, and slightly higher than the values found for oligoacenes^{16,17} or functionalized derivatives.¹⁸ On the other hand, the torsional barrier height for the rotation of the central arene ring of **1** is less than 0.03 eV,¹⁹ suggesting its free rotation at room temperature and being a rather stringent test for theoretical methods.

The conclusions achieved in this work should be applicable to closely related molecules that may also be used as molecular wires if charged or if they experience an externally applied electric field. The application of an external electric field, as normally found in molecular-based device applications, is not expected to modify the calculated values of the parameters as shown in previous studies of internal reorganization energies²⁰ and torsional barrier heights²¹ and thus will not be studied here. Admittedly, several derivatives of our prototype molecule may be used as single-molecule junctions or self-assembled monolayers, either by terminating both ends by other chemical group

* To whom correspondence should be addressed. E-mail: jc.sancho@ua.es.

† E-mail: aj.perez@ua.es.

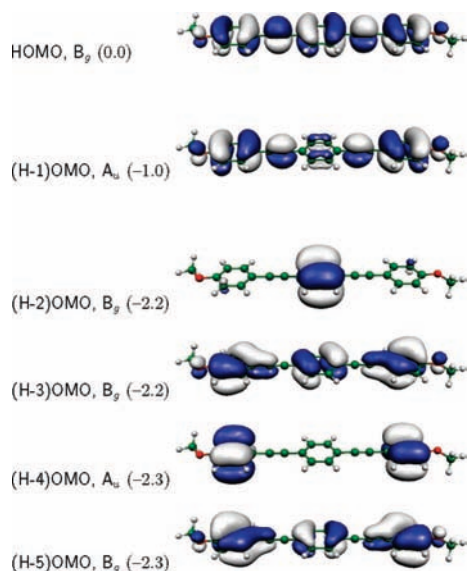


Figure 2. Contour plots of the highest occupied molecular orbitals at the RHF ground-state optimized geometry; their symmetry label and their relative energy (in eV) with respect to the HOMO level are also included.

(thiol, for instance) to allow the binding to a substrate or by substituting the central benzene ring with a nitro or amino groups. However, these functional modifications are expected to produce only small changes in the referred properties.

The outline of the paper is the following. We start in section 2 by describing the methods used in the calculations. Section 3 is devoted to assess these methods on the benchmark molecule, while section 4 analyzes the results in detail to propose further corrections for greater accuracy. The conclusions will be finally outlined in section 5.

2. Computational Methodology

2.1. Ab Initio Calculations. Complete active space self-consistent field (CASSCF) calculations,²² as implemented in the GAMESS package,²³ were done to systematically introduce static correlation effects.²⁴ A calculation of this type is normally termed CASSCF(N,M), where N and M are, respectively, the numbers of electrons and the number of orbitals included in the active space. This wave function may be further used as the reference function for a second-order perturbation correction,²⁵ which is thus referred to as a CASSCF(N,M)-MRMP2 calculation.^{26,27} Unfortunately, large active spaces are beyond the current computational capabilities of most codes due to the very demanding scaling of the calculations with respect to the active space, despite the computational strategies currently pursued to apply these methods more efficiently to large systems.^{28–30} Hence, a truncated active space must always be chosen in order to reduce as much as possible the number of the corresponding configuration state functions (CSF) but still include those which are most important for the problem at hand. Therefore, a pair of meaningful active spaces of fully π character were selected according to the relative energies and the character of the occupied orbitals and their complementary virtual orbitals, obtained at the Restricted Hartree–Fock (RHF) level. We first built a nearly minimal space (4,4) by adding to the highest occupied and lowest unoccupied molecular orbitals (HOMO and LUMO, respectively) the (H–1)OMO and (L+1)UMO orbitals. We also considered next a larger (12,12) active space formed by all of the energetically close active valence π orbitals. The relevant occupied molecular orbitals are shown in Figure 2. Note

that extending the active space would need the inclusion of deepest orbitals lying energetically more than 1 eV below the last orbital shown. Furthermore, the next B_u and A_g orbitals cannot be strictly considered part of the π space since they represent combinations of the p orbitals of the acetylenic groups and thus lie in the plane of symmetry of the molecule. Since analytical gradients are only available for the CASSCF method, the perturbation is thus treated as a single-point correction. The cc-pVDZ basis sets were used according to the frozen core calculations performed; the accuracy of the calculation is not expected to significantly vary upon further basis set extension.^{31,32}

2.2. Density Functional calculations. 2.2.1. Choice of Functional. Regarding the Kohn–Sham (KS) calculations in DFT,^{33,34} as implemented in the ORCA package,³⁵ the expression we adopt here to systematically introduce the exact exchange HF-like energy (E_x^{HF}) in a general fashion is

$$E_{xc}^{\text{hybrid}}[\rho] = w_{\text{HF}}E_x^{\text{HF}} + (1 - w_{\text{HF}})E_x[\rho] + E_c[\rho] \quad (2)$$

where $E_i[\rho]$ represents the exchange ($i = x$) or correlation ($i = c$) density functional. Note that for $w_{\text{HF}} = 0$, we recover the local density approximation (LDA) or semilocal frameworks as the generalized gradient approximation (GGA) and further extensions therein (*meta*-GGA). This evidences a hierarchy of methods, each one representing higher developments that incorporate more ingredients constructed from the density.³⁶ On the other hand, when $w_{\text{HF}} = 1$, a direct coupling between a correlation functional and the HF-like operator is obtained. The corresponding hybrid versions result from variation of w_{HF} in eq 2.^{37–40} Among the available expressions for exchange, we select the B88⁴¹ and the extended X⁴² functionals, both belonging to GGA, which are coupled to the LYP correlation functional.⁴³ The PBE⁴⁴ and TPSS^{45,46} exchange–correlation functionals are also considered, the latter probably being the most modern exponent of a *meta*-GGA expression. Table 1 presents the detailed composition of the exchange–correlation functionals used in this work. B3LYP-based^{47,48} results are also included since this functional is surely the most used within present day computational applications. Very dense and not-pruned grids for numerical integration of the exchange–correlation functionals were always used.

A further step in the complexity of the hybrid functionals has been recently introduced with remarkable results.^{49,50} A double-hybrid scheme, in the sense that both the exchange and correlation functionals are combined with exact expressions taken from ab initio theories, is thus proposed

$$E_{xc}^{\text{double-hybrid}}[\rho] = w_{\text{HF}}E_x^{\text{HF}} + (1 - w_{\text{HF}})E_x[\rho] + w_{\text{PT2}}E_c^{\text{PT2}} + (1 - w_{\text{PT2}})E_c[\rho] \quad (3)$$

where both E_x^{HF} and E_c^{PT2} are evaluated now with the orbitals arising from the solution of the DFT-based one-electron equations. The E_c^{PT2} perturbative term has the form

$$E_c^{\text{PT2}} = \frac{1}{4} \sum_{ia} \sum_{jb} \frac{((ialj) - (ibja))^2}{\epsilon_i + \epsilon_j - \epsilon_a - \epsilon_b} \quad (4)$$

where ij and ab refer to occupied and virtual spin orbitals, respectively, and ϵ are the corresponding orbital energies. The semiempirically obtained values for w_{HF} and w_{PT2} ^{49,51} are also gathered in Table 1. The analytic gradients for this perturbatively corrected density functionals are also recently available.⁵² Note that double-hybrids belong to a higher level in the hierarchy than GGA or *meta*-GGA.

We remark that for the double-hybrid functionals, all electrons should be correlated to be consistent with the original derivation

TABLE 1: Detailed Composition of the Exchange–Correlation Functionals Used along This Work

type	functional	w_{HF}^a	w_{PT2}^b	$E_x[\rho]$	$E_c[\rho]$
LDA	LDAX	0	0	Slater	–
	LDA	0	0	Slater	VWN
GGA	B	0	0	B	–
	BLYP	0	0	B	LYP
	B3LYP	0.20	0	B	LYP, VWN
	BHHLYP	0.50	0	B	LYP
	HF-LYP	1.00	0	–	LYP
	PBEX	0	0	PBE	–
	PBE	0	0	PBE	PBE
	PBE0	0.25	0	PBE	PBE
	PBEH	0.50	0	PBE	PBE
	HF-PBE	1.00	0	–	PBE
	XLYP	0	0	X	LYP
X3LYP	0.22	0	X	LYP	
<i>meta</i> -GGA	TPSSx	0	0	TPSS	–
	TPSS	0	0	TPSS	TPSS
	TPSS0	0.25	0	TPSS	TPSS
	TPSSH	0.50	0	TPSS	TPSS
	HF-TPSS	1.00	0	–	TPSS
double-hybrid	B2-PLYP	0.53	0.27	B	LYP
	B2T-PLYP	0.60	0.31	B	LYP
	B2K-PLYP	0.72	0.42	B	LYP

^a Weight of the HF-like exchange (hybrid functional). Formal scaling by N^4 , without further approximations, where N is the number of basis functions. ^b Weight of the perturbative term (double-hybrid functional). Formal scaling by N^5 , without further approximations, where N is the number of basis functions.

of the method. Therefore, we need to include extra functions, designed for treating core–core and core–valence correlation effects;⁵³ consequently, the cc-pCVDZ extension of the cc-pVDZ basis sets⁵⁴ was then employed. The resolution-of-the-identity (RI) approximation^{55–57} was also invoked for the double-hybrids to reduce the computational cost; this is, however, not expected to introduce any meaningful numerical error.⁵⁸

2.2.2. Empirical Parameters and Exchange Kernels within the PBE Model. We present here a summary of some of the existing modifications of the PBE exchange functional, which is known to satisfy as many formal properties and limits as possible for a GGA-based expression. The closed form of this functional prompted us to study the influence of other manipulations to improve agreement with experiments. In PBE, an enhancement factor $F_x[\rho]$ over the local exchange energy density, $\epsilon_x^{\text{LDA}} = -C_x \rho(\mathbf{r})^{1/3}$, allows one to express the functional as

$$E_x^{\text{PBE}}[\rho] = \int \rho(\mathbf{r}) \epsilon_x^{\text{LDA}} F_x[\rho] d\mathbf{r} \quad (5)$$

with

$$F_x^{\text{PBE}}[\rho] = 1 + \kappa - \frac{\kappa}{1 + (\mu/\kappa)s^2} \quad (6)$$

written in terms of the dimensionless density gradient $s = |\nabla \rho(\mathbf{r})|/[2(3\pi^2)^{1/3} \rho(\mathbf{r})^{4/3}]$. Note that if $F_x[\rho] = 1$, we recover the exchange-only LDA approximation (LDAX). The original values for the parameters ($\kappa = 0.804$ and $\mu = 0.21951$) were derived by imposing well-known constraints.⁴⁴ Other authors have proposed the same form but with values of κ and μ empirically fitted to a chosen database.^{59,60} We will focus here exclusively

TABLE 2: Computational Estimates of Hole Reorganization Energies (λ^{*+} , in meV) and the Torsional Barrier Height (ΔE_{tors} , in meV) As Calculated by Various Ab Initio Methods^a

method	λ^{*+}	ΔE_{tors}^b
HF	389	39.0
CASSCF(4,4)	276	27.9
CASSCF(4,4)-MRMP2	78	35.1
CASSCF(12,12)	276	23.6
CASSCF(12,12)-MRMP2	417	47.5
exp. ^c	300 ± 50	28.3 ± 0.2

^a All quantities are referred to the cc-pVDZ basis sets. ^b Taken from ref 124. ^c Taken from refs 14 and 19, respectively.

on κ , which is tightly related to the fulfilment of the Lieb–Oxford inequality⁶¹ and does not need a related change of any other parameter in the PBE correlation counterpart. An early modification (revPBE⁶²) sets $\kappa = 1.245$ by relaxing the Lieb–Oxford boundary. It should be also interesting to explore if a more drastic change in κ will largely impact the performance of the model.⁶³ Additionally, we will also assess if the use of a different enhancement factor, $F_x[\rho] = 1 + \kappa - \kappa e^{-(\mu/\kappa)s^2}$ but keeping unchanged $\kappa = 0.804$, has any influence (RPBE⁶⁴). Note that other physically motivated functional forms are also available,^{65–68} however, the conclusions are not expected to differ significantly.

3. Results and Discussion

The reorganization energies often depend significantly on the computational method applied,^{69,70} whether Hartree–Fock (HF), Møller–Plesset perturbation theory up to second order (MP2), or density functional theory (DFT) is selected. Additionally, when multiconfigurational methods (CASSCF) are used, the completeness of the active space might also impact the accuracy of the results. Note that in the calculation of λ^{*+} , we are neglecting embedding or intermolecular effects.^{71–73} Table 2 gathers the values for the hole (radical cation) reorganization energy, λ^{*+} , and the energy difference between the planar and highly twisted form, ΔE_{tors} , of **1**. First, HF is found to overestimate charge-induced geometrical deformations and thus the value of λ^{*+} also; on the other hand, the torsional barrier height is not so severely overestimated. The CASSCF(4,4) calculations give excellent predictions for both λ^{*+} and ΔE_{tors} , which practically match the experimental values. To further assess the influence of the active orbitals, we also examine the larger (12,12) active space, which leads to about 2×10^5 spin-adapted configuration state functions. This space is approximately of the same size as that previously used in other studies on all-trans linear oligoenes,^{74,75} short oligothiophenes,^{76,77} and porphyrins.⁷⁸ Interestingly, increasing the active space leads to a rapid convergence of both properties. However, the MP2 correction to both active spaces lacks accuracy, contrary to what would have been expected. The conclusion which seems to arise is that correlation effects must be delicately taken into account for these materials. Nonetheless, the MP2-corrected calculations are done at the corresponding CASSCF-optimized geometry; thus, the additional degree of freedom needed to accommodate the charge-induced or conformational distortions is lost. Additionally, the values now largely depend on the size of the active space. We have also performed single-reference MP2 single-point calculations at the HF-optimized geometries with similar results. Therefore, as a byproduct of our study, we think that the MP2-based results should be treated with some caution, as indicated also by other studies,^{16,79,80} while the CASSCF results of Table 2 can be confidently considered as more reliable.

TABLE 3: Computational Estimates of Hole Reorganization Energies (λ^{++} , in meV) and the Torsional Barrier Height (ΔE_{tors} , in meV) As Calculated by Various DFT Methods^a

type	functional	λ^{++}	ΔE_{tors}
LDA	LDAX	86	120
	LDA	86	121
GGA	B	95	105
	BLYP	94	114
	B3LYP	131	92.7
	BHHLYP	197	69.9
	HF-LYP	341	39.1
	PBEx	97	107
	PBE	90	112
	PBE0	136	87.8
	PBEH	192	67.4
	HF-PBE	350	39.6
	XLYP	90	115
	X3LYP	128	94.4
	<i>meta</i> -GGA	TPSSx	112
TPSS		101	110
TPSS0		141	85.6
TPSSHH		198	66.6
HF-TPSS		354	40.4
double-hybrid	B2-PLYP	130	76.6
	B2T-PLYP	142	73.5
	B2K-PLYP	160	68.0
exp. ^b		300 ± 50	28.3 ± 0.2

^a All quantities are referred to the cc-pCVDZ basis sets. ^b Taken from refs 14 and 19, respectively.

The results from the ab initio calculations will be compared next with those from DFT. We used various combinations of the functional form given by eq 2. The corresponding values for the hole reorganization energy, λ^{++} , and the torsional barrier height, ΔE_{tors} , are given in Table 3. We observe that pure functionals ($w_{\text{HF}} = w_{\text{PT2}} = 0$) belonging to the first three levels of the hierarchy (LDA, GGA, and *meta*-GGA) lead to rather similar values for both magnitudes. The use of different approximations for the exchange–correlation functional within each level (compare, for instance, the BLYP and PBE values) does not appreciably change the results. If the LDA calculations are treated as a baseline, it is true that a progressive improvement is achieved through the hierarchy, and, in fact, GGA (*meta*-GGA) is slightly better than LDA (GGA), but major breakthroughs are not obtained. We see that the final values (TPSS) are still affected by a large error (about 150 meV) with respect to the experimental value, even considering its large uncertainty of ± 50 meV. Analyzing now exchange-only DFT calculations (LDAX, B, PBEx, and TPSSx), we see how the results are only marginally affected after adding the corresponding correlation functional in a self-consistent fashion. The fact that the type of correlation functional does not improve the results is in full agreement with previous works on charged oligoacenes⁶⁹ and twisted dimeric systems,^{81–83} where it was also shown that the properties of π -conjugated systems are controlled by the weight of HF-like exchange. Thus, the main factor affecting the results is given by w_{HF} , as can be easily seen in Table 3. The fact that the error in the description of both properties becomes smaller as w_{HF} increases indicates a systematic error as the cause of the deviations. Furthermore, Table 4 shows that nothing significant is achieved through empirical manipulation of the PBE-based kernel, at the risk however of violating the Lieb–Oxford boundary. Figure 3 depicts how the values of λ^{++}

TABLE 4: Computational Estimates of Hole Reorganization Energies (λ^{++} , in meV) and the Torsional Barrier Height (ΔE_{tors} , in meV) As Calculated by Various PBE-based Models^a

functional	λ^{++}	ΔE_{tors}
PBE ($\kappa = 0.804$)	90	112
PBE ($\kappa = 0.4$)	88	118
PBE ($\kappa = 4.0$)	97	99
revPBE	93	109
RPBE	90	108
exp. ^b	300 ± 50	28.3 ± 0.2

^a All quantities are referred to the cc-pCVDZ basis sets. ^b Taken from refs 14 and 19, respectively.

smoothly evolve with the parameter w_{HF} . Particularly, the uniform evolution allows us to perfectly fit the data to a quadratic polynomial, whose optimum values for the hole reorganization energies are listed in Table 5 taking into account the experimental uncertainty. Unfortunately, the inclusion of higher and higher values of w_{HF} did not help to improve the torsional barrier height since convergence was not achieved, as shown in Figure 4. We see that for quantitative predictions of hole reorganization energies within the experimental uncertainties, the fraction of HF-like exchange needed is 70% at least, which is considerably higher than what is regularly employed in conventional hybrid functionals. Obviously, increasing the exact exchange weight might deteriorate the accuracy for thermochemical and other ground-state properties. On the other hand, HF-KS solutions (HF-LYP, HF-PBE, and HF-TPSS) give a qualitatively correct description (an upper limit) of the charge-transport parameters, which is not surprising given the aforementioned features. Note that a HF-KS approach is known to give poorer results than semilocal functionals in common applications. Therefore, it seems difficult to negotiate the need for different values of w_{HF} in different situations.⁸⁴ Finally, the orbital-dependent functionals combining second-order perturbation theory (PT2) and hybrid-like functionals do not lead to better results. Actually, the results (compare, for instance, the B3LYP and B2-PLYP values) do not vary much with respect to simpler and less costly hybrids.

4. Analysis of the Results

4.1. Self-Interaction Error and Fermi–Amaldi Corrections. The self-interaction error (SIE), caused by the all-pervasive interaction of an electron with itself, is known to be at the origin of some shortcomings which plague DFT. Particularly, an important effect of the SIE for the field of conjugated molecules is the over-stabilization of delocalized states,^{85–87} which indeed manifests in difficulties⁸⁸ for predicting a whole set of important magnitudes such as (i) reaction paths and energy barrier heights, (ii) torsion energy profiles and breaking of π conjugation, and (iii) polarizabilities, conductance, and other electric properties. Unfortunately, although SIE is easily defined for a one-electron system,⁸⁹ the corresponding extension in terms of the electronic density to larger systems is not so straightforward.⁹⁰ Note that most of the attempts to correct the SIE are made on an orbital-by-orbital framework,^{91–96} including the pioneering self-interaction correction (SIC) scheme,⁹⁷ which is an all time-consuming process with only partial success.⁹⁸ The detailed description of these schemes is beyond the scope of the present paper. Hence, despite its simple appearance, it is hard to remove the SIE in practice. Thus, we will prefer to circumvent this feature by looking at the effects

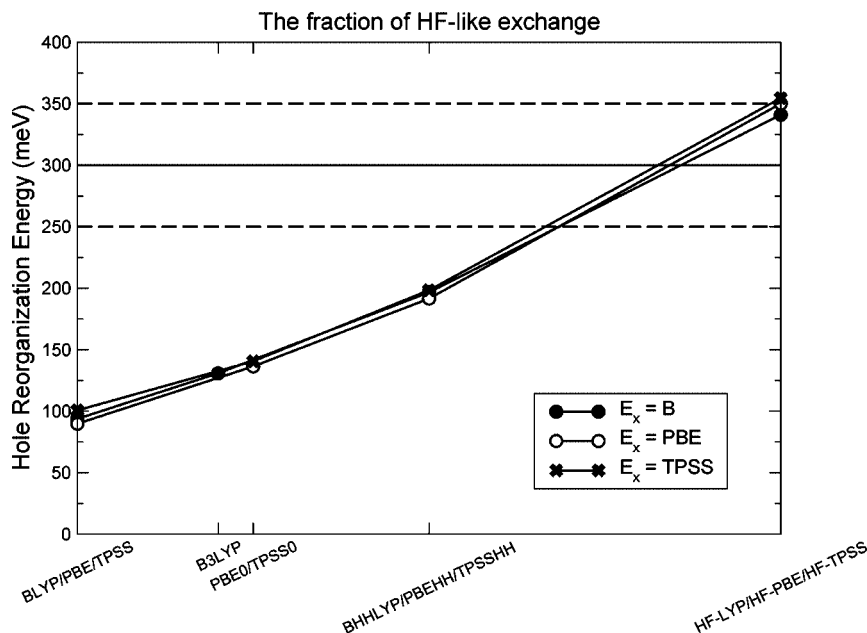


Figure 3. Evolution of the hole reorganization energy as a function of the HF-like exchange for various DFT-based models. The experimental value is indicated by a solid line with the experimental uncertainty given by the dashed lines.

TABLE 5: Optimal Value of w_{HF} for Hole Reorganization Energies

functional	w_{HF}
BLYP-based	0.871 ± 0.163
PBE-based	0.859 ± 0.148
TPSS-based	0.846 ± 0.149

^a All quantities are referred to the cc-pCVDZ basis sets.

of the SIE on the energy differences relevant to charge transport, complementing other investigations of a more theoretical nature.^{99–101}

Certainly, as we are concerned in this work with ground-state energy differences, the features of the functional derivatives of the exchange–correlation models are of less importance.¹⁰² Thus, we concentrate next in an alternative but simple approach to correct the values obtained for nonhybrid LDA, GGA, and *meta*-GGA functionals. We write the energy density functional of the system as

$$E_v[\rho] = T_s[\rho] + \int \rho(\mathbf{r})v(\mathbf{r})d\mathbf{r} + U[\rho] + E_{xc}[\rho] \quad (7)$$

where $T_s[\rho]$ is the kinetic energy functional, $\int \rho(\mathbf{r})v(\mathbf{r})d\mathbf{r}$ is the interaction of the density with the external potential $v(\mathbf{r})$, and $U[\rho]$ is the classical repulsion energy between the density and itself

$$U[\rho] = \frac{1}{2} \int \frac{\rho(\mathbf{r})\rho(\mathbf{r}')}{|\mathbf{r} - \mathbf{r}'|} d\mathbf{r}' d\mathbf{r} \quad (8)$$

The Fermi–Amaldi (FA) correction,¹⁰³ the earliest attempt to correct the self-interaction energy, simply uses an N electron average of the electron–electron repulsion energy

$$E_{xc}^{\text{FA}}[\rho] = -NU\left(\frac{\rho}{N}\right) \quad (9)$$

where N is the total number of electrons. The main advantage of this correction rests on two salient features, (i) its simplicity, although elegant in nature, and (ii) that it can be applied with unmodified versions of the most common codes. On the other hand, this correction is known to be nonsize-consistent,¹⁰⁴ as are all of the functionals explicitly depending on the total

number of electrons,¹⁰⁵ which might affect the scaling of the results with the size of the system. Note that the effect of the SIE on the bond length alternation of increasingly longer oligoenes has been recently recognized.¹⁰⁶

Table 6 reports the Fermi–Amaldi-corrected values for λ^{*+} and ΔE_{tors} . Whereas the correction works amazingly fine for the hole reorganization energy, the same is not true for the torsional barrier height. Therefore, given this state of results, the SIE seems to truly dominate the value of λ^{*+} , and even the crude Fermi–Amaldi correction is able to significantly decrease the error introduced by local (LDA) or semilocal (GGA and *meta*-GGA) functionals. The controversial behavior of this correction is attributed to a subtle difference between the two energy magnitudes. The value of λ^{*+} is greatly influenced by the existing singly occupied orbital, which is known to engender a large and systematic SIE.¹⁰⁷ The final value of ΔE_{tors} , since all of the orbitals are doubly occupied, relies however on an accurate balance of the intrapair and interpair correlation effects, as we will see next.

4.2. Static Correlation Energy Corrections. We explore now the connections between static correlation energy (SCE) and the properties of conjugated molecules, as pioneered again by the study of some conjugated oligomers.¹⁰⁸ We first recognize that it is not a simple issue to give a clear separation between electron correlation effects, as was historically stated.¹⁰⁹ The nonstatic correlation energy, also called dynamic or short-range, arises from the tight interactions between pairs of electrons. The computational determination of this correlation energy is done with high accuracy by most of the existing correlation functionals.^{110–112} Furthermore, the last generation of functionals is believed to be close to the accuracy limit that can be achieved by expressions derived within the GGA or the *meta*-GGA frameworks.^{113–115} Once we admit this feature, the remaining correlation contribution is driven by degeneracies or near-degeneracies of the system, which indeed imply the use of a multiconfigurational wave function. An unambiguous definition for the SCE is thus to include in such a wave function all CSFs which arise from all possible occupancies of the active orbitals, that is, through the well-established multiconfigurational quantum chemical methods.

Hence, for a given basis set and a selected active space, we have

$$\text{SCE}^{\text{ab initio}} = E_{\text{CASSCF}(N,M)} - E_{\text{HF}} \quad (10)$$

where $E_{\text{CASSCF}(N,M)}$ and E_{HF} are, respectively, the CASSCF(N,M) and HF total energies, which translates into the following contribution for ΔE_{tors} when the largest active space is used

$$\Delta E_{\text{tors}}^{\text{SCE}^{\text{ab initio}}} = \Delta E_{\text{tors,CASSCF}(12,12)} - \Delta E_{\text{tors,HF}} = -15.4 \text{ meV} \quad (11)$$

Let us think next about the equivalent working hypothesis in DFT. As a first-order estimate, it is customary to quantify the SCE as

$$\text{SCE}_x^{\text{DFT}} = E_x[\rho] - E_x^{\text{HF}} \quad (12)$$

since E_x^{HF} represents the exact-exchange energy, and $E_x[\rho]$, the exchange energy contribution to the DFT energy (see eq 2), is believed to represent effectively not only exchange but also molecular static correlation. The underlying reasons behind this definition are well-established in the literature.^{116–119} The corresponding transcription to ΔE_{tors} is

$$\Delta E_{\text{tors}}^{\text{SCE}_x^{\text{DFT}}} = \Delta E_{\text{tors},x}[\rho] - \Delta E_{\text{tors},x}^{\text{HF}} \quad (13)$$

which amounts (in meV) to 65.6, 68.4, and 64.8 for the B, PBEx, and TPSSx exchange functionals, respectively. Comparing $\Delta E_{\text{tors}}^{\text{SCE}^{\text{ab initio}}}$ with $\Delta E_{\text{tors}}^{\text{SCE}_x^{\text{DFT}}}$, we see that eq 12 leads to an overestimation of the SCE contribution to the torsional barrier height by an almost constant quantity of about 80 meV (≈ 2 kcal/mol, twice the so-called “chemical accuracy”), which is on the same order as the global error obtained by nonhybrid functionals (see Table 3). Thus, the difference

$$\epsilon_{\text{SCE}} = \text{SCE}^{\text{ab initio}} - \text{SCE}_x^{\text{DFT}} \quad (14)$$

represents the correction to eq 12 needed to remove any spurious SCE contribution to the DFT energy. The correction to the torsional barrier reads, accordingly

$$\Delta \epsilon_{\text{tors}}^{\text{SCE}} = \Delta E_{\text{tors}}^{\text{SCE}^{\text{ab initio}}} - \Delta E_{\text{tors}}^{\text{SCE}_x^{\text{DFT}}} \quad (15)$$

Equation 15 can be used to correct a functional with $w_{\text{HF}} = 0$. We now look for a correction valid also when $w_{\text{HF}} \neq 0$. If the overestimation of the torsional barrier height is found to linearly decrease after the introduction of a higher w_{HF} , we may revert the reasoning and correct the values obtained with a hybrid functional by $(1 - w_{\text{HF}})\Delta \epsilon_{\text{tors}}^{\text{SCE}}$. The final values (SCE-corrected) are thus obtained as

$$\Delta E_{\text{tors,SCE}} = \Delta E_{\text{tors}} - (1 - w_{\text{HF}})\Delta \epsilon_{\text{tors}}^{\text{SCE}} \quad (16)$$

and are presented in Table 7. Remarkably, the torsional barrier height predicted by all of the DFT methods ranges between 25 and 34 meV, in close agreement with the experimental result.

We now extend the previous set of ideas to the other parameter (λ^{*+}) entering into the model, which is mainly affected by the self-interaction error (SIE), as established in the preceding section. It is also known that the SIE haphazardly mimics static correlation effects.^{120–122} For an electron pair, the SIE introduced by local or semilocal functionals can partly compensate for the lack of static correlation energy between two electrons. Once we establish this connection, we thus borrow the same procedure derived above for ΔE_{tors} to correctly account for SCE-derived contributions. In such a way, the corrected λ^{*+} is calculated as

$$\lambda_{\text{SCE}}^{*+} = \lambda^{*+} - (1 - w_{\text{HF}})\Delta \epsilon_{\lambda}^{\text{SCE}} \quad (17)$$

where $\Delta \epsilon_{\lambda}^{\text{SCE}}$ is given by

$$\Delta \epsilon_{\lambda}^{\text{SCE}} = \lambda_{\text{SCE}^{\text{ab initio}}}^{*+} - \lambda_{\text{SCE}_x^{\text{DFT}}}^{*+} \quad (18)$$

with

$$\lambda_{\text{SCE}^{\text{ab initio}}}^{*+} = \lambda_{\text{CASSCF}(12,12)}^{*+} - \lambda_{\text{HF}}^{*+} \quad (19)$$

$$\lambda_{\text{SCE}_x^{\text{DFT}}}^{*+} = \lambda_{E_x[\rho]}^{*+} - \lambda_{E_x^{\text{HF}}}^{*+} \quad (20)$$

Comparing the last two quantities, we see how the SCE contribution to the hole reorganization energy is underestimated by DFT methods by about 180 meV (≈ 4 kcal/mol), which is again on the same order as the global error obtained by nonhybrid functionals (see Table 3). The corrected values are

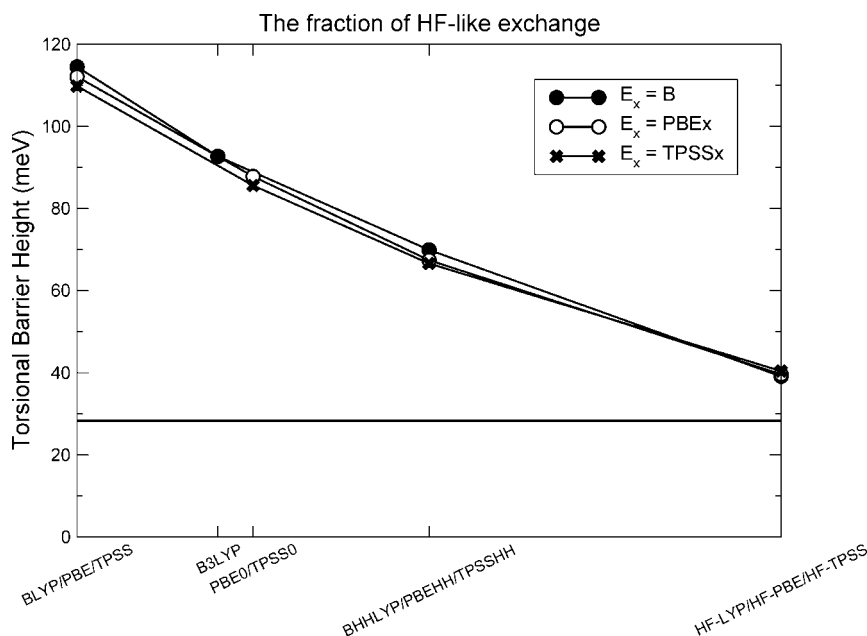


Figure 4. Evolution of the torsional barrier height as a function of the HF-like exchange for various DFT-based models. The experimental value is indicated by a solid line.

TABLE 6: Corrected (see text for details) Computational Estimates of Hole Reorganization Energies (λ^{++} , in meV) and the Torsional Barrier Height (ΔE_{tors} , in meV) As Calculated by Various Nonhybrid DFT methods^a

functional	λ_{FA}^{++}	$\Delta E_{\text{tors, FA}}$
LDA	335	245
BLYP	263	248
PBE	269	230
TPSS	288	247
exp. ^b	300 ± 50	28.3 ± 0.2

^a All quantities are referred to the cc-pCVDZ basis sets. ^b Taken from refs 14 and 19, respectively.

TABLE 7: Corrected (see text for details) Computational Estimates of Hole Reorganization Energies (λ^{++} , in meV) and the Torsional Barrier Height (ΔE_{tors} , in meV) As Calculated by Various DFT Methods^a

functional	$\lambda_{\text{SCE}}^{++}$	$\Delta E_{\text{tors, SCE}}$
LDA	276	24.8
BLYP	275	33.5
B3LYP	276	27.9
BHHLYP	287	29.4
PBE	270	28.3
PBE0	271	25.0
PBEHH	281	25.5
TPSS	265	29.6
TPSS0	264	25.4
TPSSHH	281	26.5
exp. ^b	300 ± 50	28.3 ± 0.2

^a All quantities are referred to the cc-pCVDZ basis sets. ^b Taken from refs 14 and 19, respectively.

collected in Table 7, all ranging between 264 and 287 meV, in perfect agreement with the experimental result. Although somehow striking, the ambivalent character of the SIE, being at the same time a resilient error and mimicking some correlation effects, comes again to light¹²³ in the context of a charge-transport mechanism.

5. Concluding Remarks

We have investigated by means of ab initio multiconfigurational and DFT calculations the influence of subtle electronic effects, such as static correlation and self-interaction energy, on the hole-transport properties of a semiconducting molecular wire. Since the self-interaction error of the unpaired electrons is known to mimic static correlation effects in DFT, many fundamental properties of conjugated molecules are expected to be affected as well. We expect that the same entanglement between these physical effects holds true in other organic materials. The extent to which the hole reorganization energies and torsional barrier heights are expected to be influenced by these effects when calculated by DFT mainly depends on a correct description of the static correlation energy. It has been shown that the magnitude of the modifications needed by DFT calculations to correctly account for this depends on two factors, namely, the weight of the HF-like exchange introduced into the hybrid functionals and the difference between the results obtained by nonhybrids and CASSCF(N,M) calculations. To arrive at this conclusion, we have first isolated the exchange functionals as the source of the discrepancies found, with better results for higher weights of the HF-like exchange.

There are few other promising attempts to correct DFT results which might improve the agreement with respect to experimental values, namely, empirical localized orbital correction models and averaged self-interaction corrections. We think, however,

that a more systematic way of eliminating the SIE-related problems would involve the use of an exact-exchange model coupled with a compatible correlation functional, which may represent a major step forward for further applications in organic electronics and nanotechnology. Note that, independent of the above prescriptions for DFT calculations, the multiconfigurational calculations seems to be a robust method by themselves for accurate calculations on conjugated molecular systems and are rather a time investment; thus, SIE-corrected DFT calculations will be reasonable as long as the computational cost is still significantly smaller than that of the multiconfigurational correlated calculations.

Acknowledgment. This work is supported by the “Ministerio de Educación y Ciencia” of Spain and the “European Regional Development Fund” through Project CTQ2007-66461/BQU. The two authors also thank the “Ministerio de Educación y Ciencia” of Spain for a research contract under the “Ramón y Cajal” program and the “Generalitat Valenciana” for further economic support.

References and Notes

- Galperin, M.; Ratner, M. A.; Nitzan, A. *Nano Lett.* **2005**, *5*, 125.
- Yeganeh, S.; Galperin, M.; Ratner, M. A. *J. Am. Chem. Soc.* **2007**, *129*, 13313.
- Bredás, J. L.; Beljonne, D.; Coropceanu, V.; Cornil, J. *Chem. Rev.* **2004**, *104*, 4971.
- Coropceanu, V.; Cornil, J.; da Silva Filho, D. A.; Olivier, Y.; Silbey, R.; Bredás, J. L. *Chem. Rev.* **2007**, *107*, 926.
- Grozema, F. C.; Siebbeles, L. D. A. *Int. Rev. Phys. Chem.* **2008**, *27*, 87.
- Moro, G.; Scalmani, G.; Cosentino, U.; Pitea, D. *Synth. Met.* **2000**, *108*, 165.
- Geskin, V. M.; Dkhissi, A.; Brédas, J. L. *Int. J. Quantum Chem.* **2003**, *91*, 350.
- Zade, S. S.; Bendikov, M. *Chem.—Eur. J.* **2008**, *14*, 6734.
- Sancho-García, J. C. *Chem. Phys. Lett.* **2007**, *439*, 236.
- Aviram, A.; Ratner, M. A. *Chem. Phys. Lett.* **1974**, *29*, 277.
- Reed, M. A.; Zhou, C.; Muller, C. J.; Burgin, T. P.; Tour, J. M. *Science* **1997**, *278*, 252.
- Tour, J. M. *Molecular Electronics*; World Scientific: Singapore, 2003.
- Balzani, V.; Credi, A.; Venturi, M. *Molecular Devices and Machines*; Wiley-VCH: Weinheim, Germany, 2004.
- Robey, S. W.; Cizek, J. W.; Tour, J. M. *J. Phys. Chem. C* **2007**, *111*, 17206.
- Malagoli, M.; Bredás, J.-L. *Chem. Phys. Lett.* **2000**, *327*, 13.
- Gruhn, N. E.; da Silva Filho, D. A.; Bill, T. G.; Malagoli, M.; Coropceanu, V.; Kahn, A.; Bredás, J. L. *J. Am. Chem. Soc.* **2002**, *124*, 7918.
- Malagoli, M.; Coropceanu, V.; da Silva Filho, D. A.; Brédas, J. L. *J. Chem. Phys.* **2004**, *120*, 7490.
- da Silva Filho, D. A.; Kim, E.-G.; Bredás, J. L. *Adv. Mater.* **2005**, *17*, 1072.
- Greaves, S. J.; Flynn, E. L.; Fitcher, E. L.; Wrede, E.; Lydon, D. P.; Low, P. J.; Rutter, S. R.; Beeby, A. *J. Phys. Chem. A* **2006**, *110*, 2114.
- Sancho-García, J. C.; Horowitz, G.; Brédas, J. L.; Cornil, J. *J. Chem. Phys.* **2003**, *119*, 12563.
- Zhao, J.; Li, P.; Li, Y.; Huang, Z. *J. Mol. Struct.: THEOCHEM* **2007**, *808*, 125.
- Schmidt, M. W.; Gordon, M. S. *Annu. Rev. Phys. Chem.* **1998**, *49*, 233.
- Schmidt, M. W.; Baldrige, K. K.; Boatz, J. A.; Elbert, S. T.; Gordon, M. S.; Koseki, J. H. J. S.; Matsunaga, N.; Nguyen, K. A.; Su, S. J.; Windus, T. L.; Dupuis, M.; Montgomery, J. A. *J. Comput. Chem.* **1993**, *14*, 1347.
- Mok, D. K. W.; Neumann, R.; Handy, N. C. *J. Phys. Chem.* **1996**, *100*, 6225.
- Davidson, E. R.; Jarzecki, A. A. In *Recent Advances in Multi-reference Methods*; Hirao, K., Ed.; World Scientific: Singapore, 1999.
- Nakano, H. *J. Chem. Phys.* **1993**, *99*, 7983.
- Nakano, H. *Chem. Phys. Lett.* **1993**, *207*, 372.
- Grimme, S.; Waletzke, M. *Phys. Chem. Chem. Phys.* **2000**, *2*, 2075.

- (29) Rintelman, J. M.; Adamovic, I.; Varganov, S.; Gordon, M. S. *J. Chem. Phys.* **2005**, *122*, 044105.
- (30) Robinson, D.; McDouall, J. W. *J. Chem. Theory Comput.* **2007**, *3*, 1306.
- (31) Ross, B. O.; Fülischer, M.; Malmqvist, P.-A.; Merchán, M.; Serrano-Andrés, L. In *Quantum Mechanical Electronic Structure Calculations with Chemical Accuracy*; Langhoff, S. R., Ed.; Kluwer Academic Press: Dordrecht, The Netherlands, 1995.
- (32) Smith, D. M.; Barić, D.; Maksić, Z. B. *J. Chem. Phys.* **2001**, *115*, 3474.
- (33) Hohenberg, P.; Kohn, W. *Phys. Rev. B* **1964**, *136*, 864.
- (34) Kohn, W.; Sham, L. J. *Phys. Rev. A* **1965**, *140*, 1133.
- (35) Neese, F. *ORCA—An Ab-Initio, Density Functional and Semiempirical Program Package*, version 2.5.20; University of Bonn: Germany, 2006.
- (36) Perdew, J. P.; Schmidt, K. In *Density Functional Theory and Its Application to Materials*; Van Doren, V., Van Alsenoy, C., Geerlings, P., Eds.; American Institute of Physics: Melville, NY, 2001.
- (37) Becke, A. D. *J. Chem. Phys.* **1993**, *98*, 1372.
- (38) Perdew, J. P.; Ernzerhof, M.; Burke, K. *J. Chem. Phys.* **1996**, *105*, 9982.
- (39) Adamo, C.; Barone, V. *Chem. Phys. Lett.* **1997**, *274*, 242.
- (40) Staroverov, V. N.; Scuseria, G. E.; Tao, J.; Perdew, J. P. *J. Chem. Phys.* **2003**, *119*, 12129.
- (41) Becke, A. D. *Phys. Rev. A* **1988**, *38*, 3098.
- (42) Xu, X.; Zhang, Q.; Muller, R. P.; Goddard, W. A., III. *J. Chem. Phys.* **2005**, *122*, 014105.
- (43) Lee, C.; Yang, W.; Parr, R. G. *Phys. Rev. B* **1988**, *37*, 785.
- (44) Perdew, J. P.; Burke, K.; Ernzerhof, M. *Phys. Rev. Lett.* **1996**, *77*, 3865.
- (45) Tao, J.; Perdew, J. P.; Staroverov, V. N.; Scuseria, G. E. *Phys. Rev. Lett.* **2003**, *91*, 146401.
- (46) Perdew, J. P.; Tao, J.; Staroverov, V. N.; Scuseria, G. E. *J. Chem. Phys.* **2004**, *120*, 6898.
- (47) Becke, A. D. *J. Chem. Phys.* **1993**, *98*, 5648.
- (48) Stephens, P. J.; Devlin, F. J.; Chablowski, C. F.; Frisch, M. J. *J. Phys. Chem.* **1994**, *98*, 11623.
- (49) Grimme, S. *J. Chem. Phys.* **2006**, *124*, 034108.
- (50) Schwabe, T.; Grimme, S. *Phys. Chem. Chem. Phys.* **2006**, *8*, 4398.
- (51) Tarnopolsky, A.; Karton, A.; Sertchook, R.; Vuzman, D.; Martin, J. M. L. *J. Phys. Chem. A* **2008**, *112*, 3.
- (52) Neese, F.; Schwabe, T.; Grimme, S. *J. Chem. Phys.* **2007**, *126*, 124115.
- (53) Partridge, H. In *Encyclopedia of Computational Chemistry*; Schleyer, P. v. R., Ed.; Wiley: New York, 1998.
- (54) Woon, D.; Dunning, T. H. *J. Chem. Phys.* **1995**, *103*, 4572.
- (55) Vahtras, O.; Almlöf, J.; Feyereisen, M. W. *Chem. Phys. Lett.* **1993**, *213*, 514.
- (56) Weigend, F.; Häser, M. *Theor. Chem. Acc.* **1997**, *97*, 331.
- (57) Neese, F. *J. Comput. Chem.* **2003**, *24*, 1740.
- (58) Eichkorn, K.; Treutler, O.; Öhm, H.; Häser, M.; Ahlrichs, R. *Chem. Phys. Lett.* **1995**, *240*, 283.
- (59) Becke, A. D. *J. Chem. Phys.* **1996**, *85*, 7184.
- (60) Xu, X.; Goddard, W. A., III. *J. Chem. Phys.* **2004**, *121*, 4068.
- (61) Lieb, E. H.; Oxford, S. *Int. J. Quantum Chem.* **1981**, *19*, 427.
- (62) Zhang, Y.; Yang, W. *Phys. Rev. Lett.* **1996**, *80*, 890.
- (63) Odashima, M. M.; Capelle, K. *J. Chem. Phys.* **2007**, *127*, 054106.
- (64) Hammer, B.; Hansen, L. B.; Nørskov, J. K. *Phys. Rev. B* **1999**, *59*, 7413.
- (65) Adamo, C.; Barone, V. *J. Chem. Phys.* **2002**, *116*, 5933.
- (66) Wu, Z.; Cohen, R. E. *Phys. Rev. B* **2006**, *73*, 235116.
- (67) Madsen, G. K. H. *Phys. Rev. B* **2007**, *75*, 195108.
- (68) Perdew, J. P.; Ruzsinszky, A.; Csonka, G. I.; Vydrov, O. A.; Scuseria, G. E.; Constantin, L. A.; Zhou, X.; Burke, K. *Phys. Rev. Lett.* **2008**, *100*, 136406.
- (69) Sancho-García, J. C. *Chem. Phys.* **2007**, *331*, 321.
- (70) Bromley, S. T.; Illas, F.; Mas-Torrent, M. *Phys. Chem. Chem. Phys.* **2008**, *10*, 121.
- (71) Bromley, S. T.; Mas-Torrent, M.; Hadley, P.; Rovira, C. *J. Am. Chem. Soc.* **2004**, *126*, 6544.
- (72) Torras, J.; Bromley, S.; Bertran, O.; Illas, F. *Chem. Phys. Lett.* **2008**, *457*, 154.
- (73) Sancho-García, J. C.; Pérez-Jiménez, A. J. *J. Chem. Phys.* **2008**, *129*, 024103.
- (74) Kurashige, Y.; Nakano, H.; Nakao, Y.; Hirao, K. *Chem. Phys. Lett.* **2004**, *400*, 425.
- (75) Salzner, U. *J. Chem. Theory Comput.* **2007**, *3*, 219.
- (76) Rubio, M.; Merchán, M.; Pou-Américo, R.; Ortí, E. *ChemPhys Chem* **2003**, *4*, 1308.
- (77) Rubio, M.; Merchán, M.; Ortí, E. *ChemPhysChem* **2003**, *4*, 1308.
- (78) Radoń, M.; Broclawik, E. *J. Chem. Theory Comput.* **2007**, *3*, 728.
- (79) Li, X.-Y.; Tong, J.; He, F.-C. *Chem. Phys.* **2000**, *260*, 283.
- (80) Olofsson, J.; Larsson, S. *J. Phys. Chem. B* **2001**, *105*, 10398.
- (81) Sancho-García, J. C.; Brédas, J. L.; Cornil, J. *Chem. Phys. Lett.* **2003**, *377*, 63.
- (82) Sancho-García, J. C.; Cornil, J. *J. Chem. Phys.* **2004**, *121*, 3096.
- (83) Sancho-García, J. C. *J. Chem. Phys.* **2006**, *124*, 124112.
- (84) Orlova, G.; Goddard, J. D. *Mol. Phys.* **2002**, *100*, 483.
- (85) Sancho-García, J. C.; Pérez-Jiménez, A. J.; Moscardó, F. J. *Phys. Chem. A* **2001**, *105*, 10541.
- (86) Woodcock, H. L.; Schaefer, H. F., III; Schreiner, P. R. *J. Phys. Chem. A* **2002**, *106*, 11923.
- (87) Lundberg, M.; Siegbahn, P. E. M. *J. Chem. Phys.* **2005**, *122*, 224103.
- (88) Reimers, J. R.; Cai, Z.-L.; Bilić, A.; Hush, N. S. *Ann. N.Y. Acad. Sci.* **2003**, *1006*, 235.
- (89) Zhang, Y.; Yang, W. *J. Chem. Phys.* **1998**, *109*, 2604.
- (90) Mori-Sánchez, P.; Cohen, A. J.; Yang, W. *J. Chem. Phys.* **2006**, *125*, 201102.
- (91) Patchkovskii, S.; Ziegler, T. *J. Chem. Phys.* **2002**, *116*, 7806.
- (92) Legrand, C.; Suraud, E.; Reinhard, P.-G. *J. Phys. B: At. Mol. Opt. Phys.* **2002**, *35*, 1115.
- (93) Ciofini, I.; Chermette, H.; Adamo, C. *Chem. Phys. Lett.* **2003**, *380*, 12.
- (94) Tsuneda, T.; Kamiya, M.; Hirao, K. *J. Comput. Chem.* **2003**, *24*, 1592.
- (95) Vydrov, O. A.; Scuseria, G. E. *J. Chem. Phys.* **2005**, *122*, 184107.
- (96) Vydrov, O. A.; Scuseria, G. E. *J. Chem. Phys.* **2006**, *124*, 191101.
- (97) Perdew, J. P.; Zunger, A. *Phys. Rev. B* **1981**, *23*, 5048.
- (98) Kummel, S.; Kronik, L. *Rev. Mod. Phys.* **2008**, *80*, 3.
- (99) Gritsenko, O.; Ensing, B.; Schipper, P. R. T.; Baerends, E. J. *J. Phys. Chem. A* **2000**, *104*, 8558.
- (100) Gräfenstein, J.; Kraka, E.; Cremer, D. *J. Chem. Phys.* **2004**, *120*, 524.
- (101) Ruzsinszky, A.; Perdew, J. P.; Csonka, G. I.; Vydrov, O. A.; Scuseria, G. E. *J. Chem. Phys.* **2006**, *125*, 194112.
- (102) Ayers, P. W.; Morrison, R. C.; Parr, R. G. *Mol. Phys.* **2005**, *103*, 10.
- (103) Fermi, E.; Amaldi, E. *Accad. Ital. Rome* **1934**, *6*, 117.
- (104) Perdew, J. P. *Adv. Quantum Chem.* **1990**, *21*, 113.
- (105) Pérez-Jiménez, A. J.; Moscardó, F.; Sancho-García, J. C.; Abia, L. P.; San-Fabián, E.; Pérez-Jordá, J. M. *J. Chem. Phys.* **2001**, *114*, 2022.
- (106) Ciofini, I.; Adamo, C.; Chermette, H. *J. Chem. Phys.* **2005**, *123*, 121102.
- (107) Friesner, R. A.; Knoll, E. H.; Cao, Y. *J. Chem. Phys.* **2006**, *125*, 124107.
- (108) Choi, C. H.; Kertesz, M.; Karpfen, A. *J. Chem. Phys.* **1997**, *107*, 6712.
- (109) Sinanoglu, O. *Adv. Chem. Phys.* **1964**, *6*, 358.
- (110) Gritsenko, O. V.; Schipper, P. R. T.; Baerends, E. J. *J. Chem. Phys.* **1997**, *107*, 5007.
- (111) Sancho-García, J. C.; Moscardó, F. *J. Chem. Phys.* **2003**, *118*, 1054.
- (112) Valderrama, E.; Ugalde, J. M. *J. Math. Chem.* **2005**, *37*, 211.
- (113) Becke, A. D. *J. Comput. Chem.* **1999**, *20*, 63.
- (114) Cohen, A. J.; Handy, N. C. *Mol. Phys.* **2001**, *99*, 607.
- (115) Zhao, Y.; Truhlar, D. G. *Acc. Chem. Res.* **2008**, *41*, 157.
- (116) Handy, N. C.; Cohen, A. J. *Mol. Phys.* **2001**, *99*, 403.
- (117) Molawi, K.; Cohen, A. J.; Handy, N. C. *Int. J. Quantum Chem.* **2002**, *89*, 86.
- (118) Becke, A. D. *J. Chem. Phys.* **2003**, *119*, 2972.
- (119) Becke, A. D. *J. Chem. Phys.* **2005**, *122*, 064101.
- (120) Cremer, D. *Mol. Phys.* **2001**, *99*, 1899.
- (121) Polo, V.; Kraka, E.; Cremer, D. *Mol. Phys.* **2002**, *100*, 1771.
- (122) Filatov, M.; Cremer, D. *J. Chem. Phys.* **2003**, *5*, 2320.
- (123) Gräfenstein, J.; Kraka, E.; Cremer, D. *Phys. Chem. Chem. Phys.* **2004**, *6*, 1096.
- (124) Sancho-García, J. C.; Pérez-Jiménez, A. J. *Phys. Chem. Chem. Phys.* **2008**, *10*, 2308.